Path Planning of a 3-UPU Wrist Manipulator for Sun Tracking in Central Receiver Tower Systems

R.B. Ashith Shyam[1], Ghosal A[2,*]

Abstract

Heliostats capable of tracking the sun as it moves across the sky and focusing the incident solar energy on to a central receiver tower requires a two degree-of-freedom (DOF) mechanism which can orient the mirror in the desired manner. Existing two-DOF mechanism, such as the Azimuth-Elevation (Az-EL) and the Target-Aligned (T-A), have two actuators in series. It is known that during certain times of the day, the T-A configuration has less spillage losses and astigmatic aberration while at other times the Az-El configuration is better. In this paper, we propose a three-DOF parallel manipulator which can be used as a heliostat. The proposed 3-UPU, three-DOF parallel manipulator, has a fixed point about which the mirror can rotate about three axes. Since only two DOF are required to track the sun, the 3-UPU is a redundant system. We propose a strategy to use this redundancy and electronically reconfigure the 3-UPU to achieve the Az-El and T-A configurations thus achieving the advantages of both. As the motion of the sun is precisely known for a known location, time and day of the year, numerical simulations done a priori provide the conditions for switching.

Keywords: Heliostat, 3-UPU wrist, Sun tracking, Parallel manipulator, Central receiver, PID control

1. Introduction

From the time parallel manipulators were first introduced by [1, 2], it has been known that they provide high structural rigidity and more accurate positioning and orientation of the end-effector or the moving platform[3]. The increased rigidity is due to the fact that the moving platform is supported at multiple points thereby the external load is shared. The increased accuracy is due to the fact that the positioning and pointing error of the end-effector is a

*Corresponding author

Email addresses: shyamashi@gmail.com (R.B. Ashith Shyam), asitava@mecheng.iisc.ernet.in (Ghosal A)

URL: http://www.mecheng.iisc.ernet.in/~asitava/ (Ghosal A)

[1]Research Scholar, Mechanical Engineering, Indian Institute of Science, Bangalore

[2]Professor, Mechanical Engineering, Indian Institute of Science, Bangalore

function of the largest error in any actuator and *not* the sum of the errors as in a serial arrangement. Due to these inherent advantages, parallel manipulators have been extensively used in flight simulators, precision manufacturing, pointing devices, medical applications, and, more recently, in video games. In harvesting solar energy, one approach is to reflect the incident solar radiation by mirrors on to a stationary central receiver (CR). At the central receiver, the reflected solar thermal radiation from several such mirrors are converted to electricity. As the Earth rotates during the day and around the sun, the sun traces a well-defined path in the sky and to continuously reflect the solar radiation, the mirror has to rotate about two axis. The device including the mirror and the actuators required to rotate the mirror assembly is called a heliostat and traditionally the two rotation axis of a heliostat are in series. In the well-known Azimuth-Elevation (Az-El) arrangement, as the name implies, the mirror is rotated about the elevation and the azimuth axis. In another configuration, the mirror is rotated about a line connecting the mirror centre to the stationary receiver centre and about the elevation – this is known as the Target-Aligned (T-A) or the Spinning-Elevation arrangement. The pointing accuracy requirement for a typical heliostat is 2-3 mrad and the heliostat is expected to track the sun in the presence of wind and gravity loading (see reference [4] for more details on heliostat and sun tracking). Since precise positioning of the end-effector and enhanced rigidity (mirror in our case) are the well-known advantages of a parallel manipulator, in this paper, we propose the use of a three-degree-of-freedom parallel manipulator for sun tracking in concentrated solar power systems. The more precise positioning capability can allow the use of low precision and low cost actuators. The enhanced inherent rigidity will allow the use of larger mirrors which for a desired output from a solar plant implies less number of heliostats and less number of actuators in the field. The enhanced rigidity also implies that lesser amount of structural supporting material need to be used to withstand wind and external loading.

There have been a few attempts to use parallel manipulators in sun tracking. In the work by [5], a two degree-of-freedom parallel manipulator called the U-2PUS has been developed for photo-voltaic (PV) systems. The author claims that this manipulator is ideal for photo-voltaic systems in latitudes from 0 to 50°. This parallel manipulator could be used for photo-voltaic systems but cannot be used for central receiver (CR) systems since in a field with photo-voltaic panels, all the PV panels are tracked in a similar manner. There is no reflection of the incident solar radiation and the conversion to electricity takes place in the PV panel itself. The location of the PV panels in the field do not play any part as the Sun's rays are parallel everywhere. For central receiver systems, the heliostats at different locations in the field will have different motion if the incident energy is to be reflected to a central receiver. Mathematically, it can be shown that there are more unknowns than equations available in the U-2PUS parallel manipulator system and hence it cannot be used in a CR system. A four degree-of-freedom parallel manipulator is proposed for sun-tracking in [6]. In this work, the collector which is initially kept high above the ground is allowed to fall down in a controlled manner under the influence of gravity thereby

attaining the required orientation. One major drawback of this manipulator is that it casts its own shadow on the collector and no prototype has been made to check the veracity of the claims. Google's Heliostat Optical Simulation Tool (HOpS) [7] is an attempt to do sun tracking in CR systems by the use of cable attached mirrors. Although there are some advantages to the system, this can be used only in places where the wind speeds are very low. Several other two degree-of-freedom (DOF) spherical mechanisms [8, 9, 10, 11] for application specific purposes such as camera orientation, scanning spherically shaped items etc. are described in literature but none of these have been shown to be capable of tracking the sun for central receiver systems. In a CR system, the heliostats cost about 40-50% of the total installation cost [21]. The main reason for this is the cantilever kind of support structure provided for the mirror. This is one of the possible areas where cost reduction could be achieved by using platform type manipulator.

A new type of tracking strategy which is independent of latitude has been proposed in [22]. The authors claim to have introduced some advantages in mechatronic control schemes, high optical efficiency by operating the heliostat at a very narrow range of incident angles. Another interesting strategy called an integer linear programming is developed for optimizing the aiming strategy [23] and thus to control the spike on the receiver aperture temperature thereby preventing its damage. The pitch-roll and slope-drive tracking mechanisms [27, 28, 29, 30] are gaining popularity and has been employed in the CSIRO and Stellio heliostats.

In this work, the focus is on CR systems and we propose a parallel manipulator, viz., the 3-UPU wrist that can be used for sun tracking in CR systems without any of the above mentioned disadvantages. The 'U' denotes a two-DOF Hooke joint, the 'P' denotes single DOF a prismatic or sliding joint. In the parallel manipulator, the 'P' joint is actuated and the other joints are not actuated or are passive. In addition, the 3-UPU can be reconfigured to be used either in Azimuth-Elevation (Az-El) or in the Target-Aligned (T-A or spinning-elevation) method thus combining the advantages of both by simply changing software and control strategy and *does not* require any change in the hardware. The 3-UPU wrist can thus be operated in a mode which gives the best performance in terms of spillage losses or astigmatism at a particular time of the day or a date in the year. In the parallel configuration, linear actuators are used. The motion of the prismatic (P) joints or the stroke of the linear actuators are computed using inverse kinematics algorithms and adjusted with respect to time to achieve the orientation required for sun tracking. The parallel manipulator requires three actuators as opposed to two in the Az-El and T-A configurations. However, since the support material is less [12] or larger mirrors can be used and less expensive and less accurate linear actuators can be used, the overall cost of the plant is expected to be less.

The paper is organized as follows: Section 2 gives the kinematics of the 3-UPU wrist and the rotation matrix for both the Az-EL and T-A heliostat are obtained. From a desired rotation matrix, the actuations at the P joints are computed. In section 3, extensive simulations are carried out for Bangalore and

Rajasthan, India on the feasibility of using a 3-UPU wrist as a sun tracker in CR systems. Section 4 shows the prototype design, the control strategy, the actual sun tracking experiment carried out and the observations made during the experiment. Finally, section 5 summarizes the work done and gives an insight into the future directions.

2. Kinematics of the 3-UPU wrist manipulator

The 3-UPU manipulator has a fixed base and a moving platform connected together by three legs having joints in the order universal-prismatic-universal (UPU). The conditions which have to be satisfied for making a 3-UPU manipulator to be a wrist are listed in [13] and the kinematics equations of the 3-UPU wrist manipulator is given in reference[14]. The 3-UPU wrist manipulator is

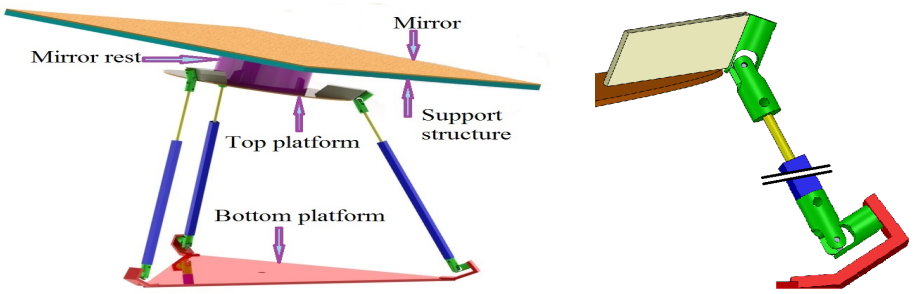

(a) CAD model of the 3-UPU wrist

(b) A close-up view of the arrangement of the joints

Fig. 1: 3-UPU heliostat and its joints

capable of performing finite spherical motions about a fixed point when the prismatic joints are actuated. For sun tracking, the fixed point should be carefully chosen so that it falls above the moving platform at the top. As shown in section 2, by using suitable attachments (mirror rest as described in this work), the mirror centre and the fixed point are made to coincide with each other. This design makes the mirror rotate about the fixed point just like in a serial Az-El or T-A arrangements as one can make two consecutive Euler rotations about a point for sun tracking.

The schematic diagram of the 3-UPU wrist manipulator is shown in Fig 2. The global or fixed co-ordinate system with its origin at O has axes OX, OY and OZ pointing towards local East, local North and Zenith directions respectively. The Z axis of the global co-ordinate system passes through the centre of the vertical receiver tower. The base co-ordinate system, {B} having axes x_b, y_b and z_b has its origin at O_1 and is at a radius, R, from O and at an angle ψ with respect to the OX axis. The co-ordinate system at the top platform, {M} has its origin at G and has axes x_m, y_m and z_m. The symbols U_{bi} and U_{ti} $(i = 1, 2, 3)$ denote the universal joints at the base and top, respectively.

Without loss of generality, the triangles formed by U_{bi} and U_{ti} can be considered to be equilateral triangles whose circum-radii are r_b and r_p, respectively. The degrees of freedom of the manipulator can be found out by using the well-known Grübler - Kutzbach equation [18]:

$$DOF = \lambda(N - J - 1) + \Sigma F_i, \tag{1}$$

where λ is 6 for spatial and 3 for planar motion, N is the number of links including the fixed link, J is the number of joints and F_i is the degrees of freedom of i^{th} joint and is 3 or in other words three actuators are needed. From the notion of the latitude, longitude, time and day of the year, the Sun vector or the ray pointing towards the Sun can be found out using the Eqn. 2 [12]

$$\overrightarrow{GN} = \frac{\overrightarrow{GS} + \overrightarrow{GR}}{||\overrightarrow{GS} + \overrightarrow{GS}||} \tag{2}$$

where $\overrightarrow{GS}$ and $\overrightarrow{GR}$ are the unit vectors pointing to the Sun and the receiver centre respectively as shown in Fig 2. The calculations required to find the transformation matrix for Sun tracking in the Az-El or the T-A mode can be obtained and is described in the next section.

2.1. Rotation matrix for Az-El case

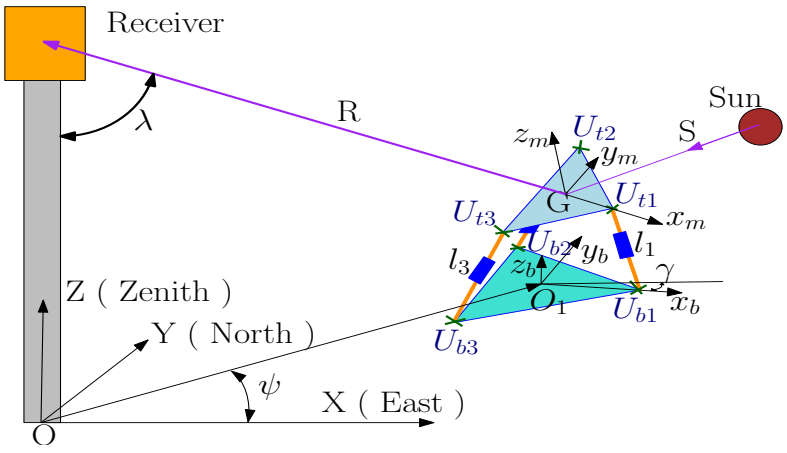

Fig. 2: Schematic of the 3-UPU

At the end of each day's operation, the mirror would be brought back to home position or stowed which refers to an orientation where the plane of the mirror is parallel to the ground plane with the mirror coordinate system $(x_m - y_m - z_m)$ being parallel to the global coordinate system. Then for an Az-El heliostat, the two Euler rotations required to track Sun (early morning next day) and reflect the rays to the receiver are

1. Rotation about Z by an angle θ_{Az} where θ_{Az} is the angle made by the projection of heliostat normal with the X axis..
2. Rotation about y_m by an angle $(\frac{\pi}{2} - \theta_{El})$ where θ_{El} is the angle made by the heliostat normal with the ground plane.

Hence, the rotation matrix becomes

$$R_{Az-El} = \begin{bmatrix} \cos\theta_{Az}\sin\theta_{El} & -\sin\theta_{Az} & \cos\theta_{Az}\cos\theta_{El} \\ \sin\theta_{Az}\sin\theta_{El} & \cos\theta_{Az} & \sin\theta_{Az}\cos\theta_{El} \\ -\cos\theta_{El} & 0 & \sin\theta_{El} \end{bmatrix} \tag{3}$$

In such a rotation, the y_m axis of the mirror coordinate system would still lie on a plane parallel to the XY plane and it is verified by noting that the (3,2) element of the rotation matrix, R_{Az-El}, is zero. The third column of the rotation matrix are the direction cosines of the normal $\overrightarrow{GN}$ which is given by Eqn. 2 and is completely known. The other two columns of the rotation matrix are found out by carrying out suitable inverse trigonometric calculations.

The above same rotation matrix can also be found out using the following approach – Denoting the columns of a general rotation matrix by $(n_1, n_2, n_3)^T$, $(o_1, o_2, o_3)^T$ and $(a_1, a_2, a_3)^T$ as its first, second and third column, respectively, for Az-El rotation, we have $o_3 = 0$ and $(a_1\ a_2\ a_3)^T$ is obtained from Eqn. 2.

Thus we have five equations from the orthogonality conditions (see Eqn. 4) from the columns of the rotation matrix and five unknowns, viz., n_1, n_2, n_3, o_1 and o_2.

$$n_1^2 + n_2^2 + n_3^2 = 1 \tag{4a}$$
$$o_1^2 + o_2^2 = 1 \tag{4b}$$
$$n_1a_1 + n_2a_2 + n_3a_3 = 0 \tag{4c}$$
$$n_1o_1 + n_2o_2 = 0 \tag{4d}$$
$$o_1a_1 + o_2a_2 = 0 \tag{4e}$$

Solving these equations for the unknowns, we get

$$n_3 = \sqrt{\frac{a_1^2 + a_2^2}{a_1^2 + a_2^2 + a_3^2}}; \qquad n_2 = -n_3\ \frac{a_3a_2}{a_1^2 + a_2^2}; \qquad n_1 = n_2\ \frac{a_1}{a_2};$$
$$o_2 = \sqrt{\frac{a_1^2}{a_1^2 + a_2^2}}; \qquad o_1 = -o_2\frac{a_2}{a_1};$$

2.2. Rotation matrix for Target-Aligned heliostat

The T-A equations for sun tracking have been developed and is given in various references [15, 16, 17]. In the T-A configuration, one of the axes of

rotation will be coincident with the reflected ray ($\overrightarrow{GR}$) and the other axis is perpendicular to the reflected ray and lies in the plane of the mirror. Thus the heliostat spins about $\overrightarrow{GR}$ by θ_{sp} (spinning angle) and rotates about y_m by θ_{el} (elevation angle). For mounting the heliostat in this special arrangement, two Euler rotations have to be performed initially, the first about Z axis by an angle ψ and then about y_m by an angle $-\lambda$. After these two consecutive rotations, the normal to the mirror and the reflected ray will become coincident. Now the rotation matrix for the T-A heliostat will become as shown in Eqn. 5

$$\begin{bmatrix} c_\psi c_\lambda c_{\theta_{sp}} c_{\theta_{el}} - s_\psi s_{\theta_{sp}} c_{\theta_{el}} + c_\psi s_\lambda s_{\theta_{el}} & -c_\psi c_\lambda s_{\theta_{sp}} - s_\psi c_{\theta_{sp}} & c_\psi c_\lambda c_{\theta_{sp}} s_{\theta_{el}} - s_\psi s_{\theta_{sp}} s_{\theta_{el}} - c_\psi s_\lambda c_{\theta_{el}} \\ s_\psi c_\lambda c_{\theta_{sp}} c_{\theta_{el}} + c_\psi s_{\theta_{sp}} c_{\theta_{el}} + s_\psi s_\lambda s_{\theta_{el}} & -s_\psi c_\lambda s_{\theta_{sp}} + c_\psi c_{\theta_{sp}} & s_\psi c_\lambda c_{\theta_{sp}} s_{\theta_{el}} + c_\psi s_{\theta_{sp}} s_{\theta_{el}} - s_\psi s_\lambda c_{\theta_{el}} \\ s_\lambda c_{\theta_{sp}} c_{\theta_{el}} - c_\lambda s_{\theta_{el}} & -s_\lambda s_{\theta_{sp}} & s_\lambda c_{\theta_{sp}} s_{\theta_{el}} + c_\lambda c_{\theta_{el}} \end{bmatrix} \quad (5)$$

where c_z, s_z represents the cosine and sine of the respective angles given by z. As in the Az-El heliostat, the normal $\overrightarrow{GN}$ and hence the third column of the rotation matrix is known. The angles ψ and λ (see Fig 2) are also known from the prior knowledge of heliostat location in the field. Thus the first and second columns of the rotation matrix can be computed.

2.3. Actuations required for the 3-UPU wrist

As mentioned earlier, the top-platform and the mirror are connected together using an attachment such that the orientation of both are the same with respect to the base. The only difference being the centre of the mirror remains at the fixed point even while executing finite spherical rotations whereas it is not the same for the top platform. Initially, both the top and bottom platforms are assumed to be parallel. Then the rotation which takes the mirror to the base is found out as mentioned in sections 2.1 and 2.2. The centre of the top platform will be at a constant distance from the mirror centre in its normal direction downwards. Using this information, the centre of the top platform is found out and hence the actuation required for the legs of 3-UPU wrist can be found out as follows:

For the 3-UPU manipulator, the co-ordinates of the U_{bi} joints with respect to $\{B\}$ are given by

$$\begin{aligned} \overrightarrow{O_1U_{b1}} &= (r_b, 0, 0)^T \\ \overrightarrow{O_1U_{b2}} &= (-\frac{1}{2}r_b, \frac{\sqrt{3}}{2}r_b, 0)^T \\ \overrightarrow{O_1U_{b3}} &= (-\frac{1}{2}r_b, -\frac{\sqrt{3}}{2}r_b, 0)^T \end{aligned}$$

and the co-ordinates of the U_{ti} joints with respect to $\{x_m, y_m, z_m\}$ are given by

$$\begin{aligned}\overrightarrow{GU_{t1}} &= (r_p, 0, 0)^T \\ \overrightarrow{GU_{t2}} &= (-\frac{1}{2}r_p, \frac{\sqrt{3}}{2}r_p, 0)^T \\ \overrightarrow{GU_{t3}} &= (-\frac{1}{2}r_p, -\frac{\sqrt{3}}{2}r_p, 0)^T\end{aligned}$$

The position vector of the top U joints with respect to the base co-ordinate system $\{B\}$ is given as

$$\begin{bmatrix}\overrightarrow{O_1U_{ti}} \\ 1\end{bmatrix} = \begin{bmatrix}T\end{bmatrix}\begin{bmatrix}\overrightarrow{GU_{ti}} \\ 1\end{bmatrix}$$

where [T] is the 4 x 4 transformation matrix which relates the mirror {M} to the base co-ordinate system {B}. The leg lengths or the actuation needed can be found out as in reference [18] and is reproduced here as given in Eqn. 6

$$l_i = ||\overrightarrow{O_1U_{bi}} - \overrightarrow{O_1U_{ti}}|| \tag{6}$$

where $i = 1, 2, 3$ and $||A||$ represents the norm of the vector described by A and U_{ti} and U_{bi} (i = 1,2,3) are the universal joints at the top and base respectively as given in Fig 2.

3. Simulation results for 3-UPU wrist

Extensive simulations have been carried out to prove that the 3-UPU wrist can indeed work in both Az-El and T-A modes. To perform the simulations a program has been developed for carrying out the simulation study for any location on the Earth's surface and for any day. For illustrative purpose, we show simulations carried out for Bangalore (12°58′13" N, 77°33′37" E) and Rajasthan (26°42′58" N, 75°41′44"E) for four days, viz., March equinox, summer solstice, September equinox and winter solstice. These four days represent the extremes of the angular tilt of the earth's rotational axis with respect to the incoming Sun rays. The height of the receiver tower varies from 43 m (IEA-CRS, Spain [4])-195 m (Crescent dunes, USA). For simulation we take the centre of the receiver aperture to be at a location $[0\ 0\ 65]^T$ m with respect to the global co-ordinate system. Although the distance of the heliostats from the tower in a surround solar field varies from a few meters to as large as a kilometer, we present the simulation results for a heliostat placed at a radial distance of 100 m and at an angle of 30° with the local east axis. From the prototyping and proof of concept point of view, anything more than 2 m in dimension would be difficult to handle and expensive. Hence the simulations parameters are chosen accordingly. The fixed point of the 3-UPU wrist is assumed to be at a height of 2 m from the bottom platform. The mirror and the receiver aperture are assumed to have a

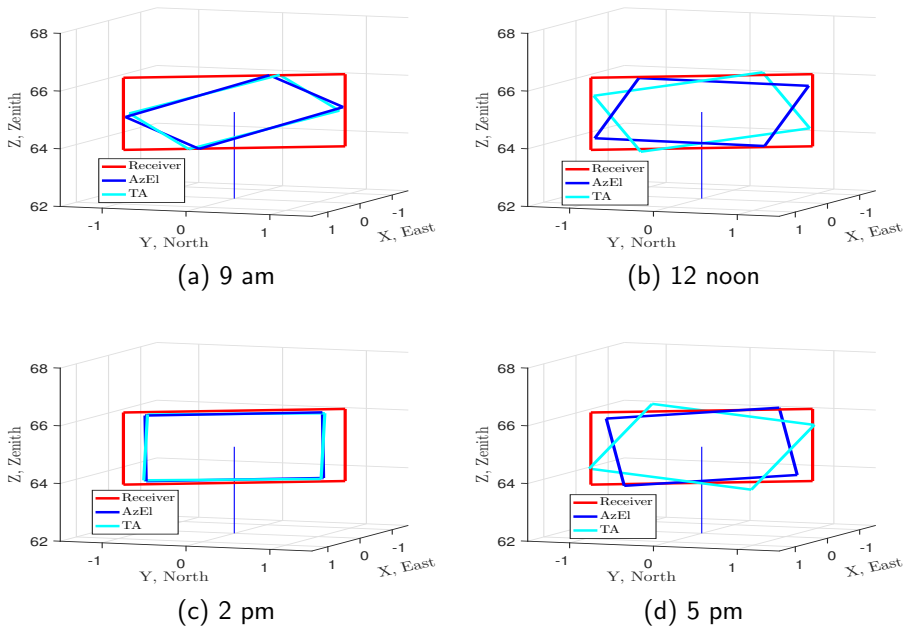

Fig. 3: The image on the receiver aperture at various time instants for March equinox for Bangalore

dimension of 2 m $\times$ 2 m and 2.5 m $\times$ 2.5 m respectively. For the simulations, the following assumptions are made:

- Atmospheric conditions like dust and other particles which reflect the Sun rays are negligible,
- The mirrors are perfectly flat, and
- At every instant of time, the Sun ray hitting the centre of the mirror goes to the centre of the receiver aperture.

Thus the ray hitting the corners of the mirror will be reflected parallel to the central ray and by tracing this ray on the receiver aperture, we can obtain the image formed at the receiver. This plot of the image on the receiver plane for a 3-UPU wrist working in Az-EL and T-A methods are shown in Fig 3. Fig 4 shows the simulation results for various time instants for March equinox in Bangalore if the 3-UPU wrist manipulator is to be used in T-A method. It is clearly understood from Fig 4d that the legs of the 3-UPU wrist intersect each other during the evening time. In order to prevent this, the rotation matrix obtained using T-A method can be multiplied by a rotation about the mirror normal so that the legs of the 3-UPU will not intersect. Fig 5 shows the modified simulation results when the T-A rotation matrix is multiplied by

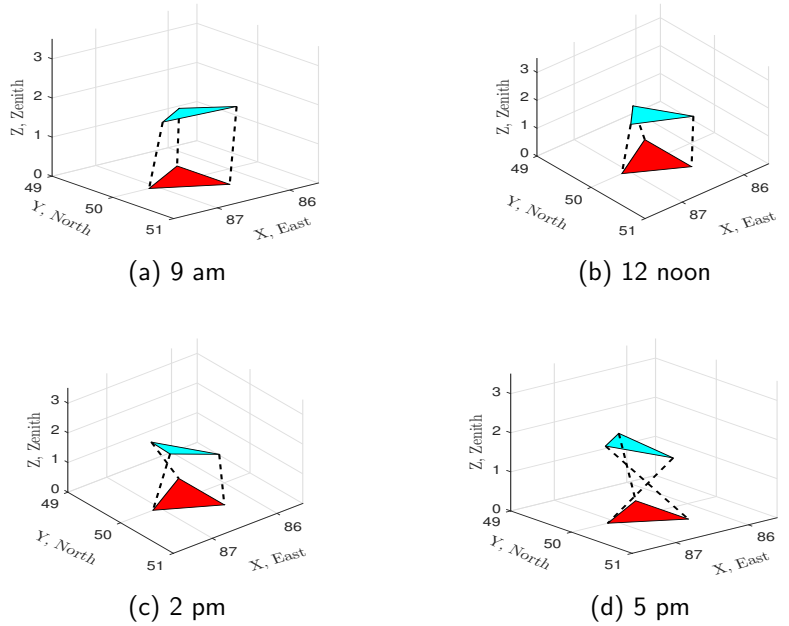

Fig. 4: Simulation of 3-UPU wrist for T-A mode for March equinox for Bangalore

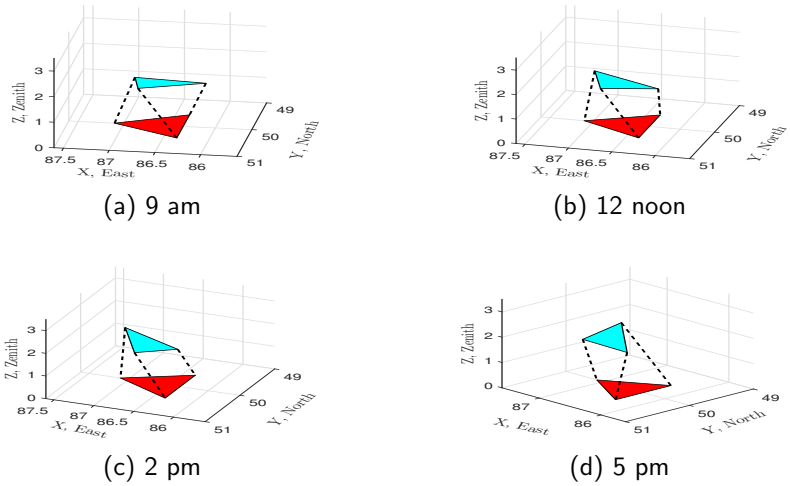

Fig. 5: Simulation of 3-UPU wrist for modified T-A mode for March equinox for Bangalore

another rotation about mirror normal by 60°. The actuations required for T-A and modified T-A are given in Fig 6. Similarly, Fig 7 gives the simulation

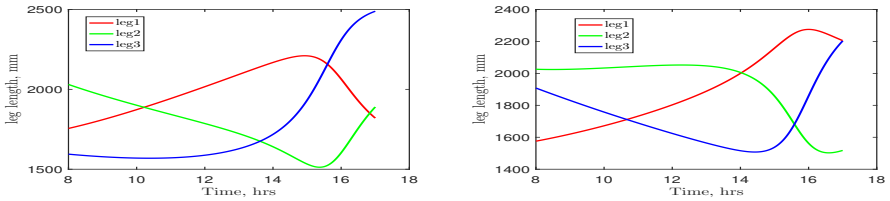

(a) T-A (b) T-A modified

Fig. 6: Actuations required for 3-UPU wrist for March equinox for Bangalore

(a) 9 am (b) 12 noon

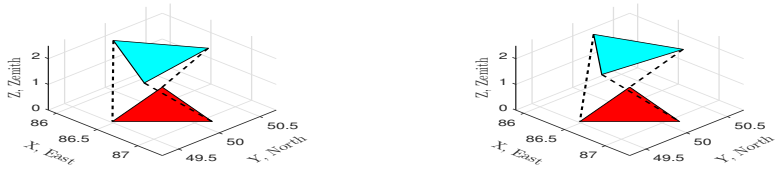

(c) 2 pm (d) 5 pm

Fig. 7: Simulation of 3-UPU wrist for modified Az-El mode for summer solstice for Rajasthan

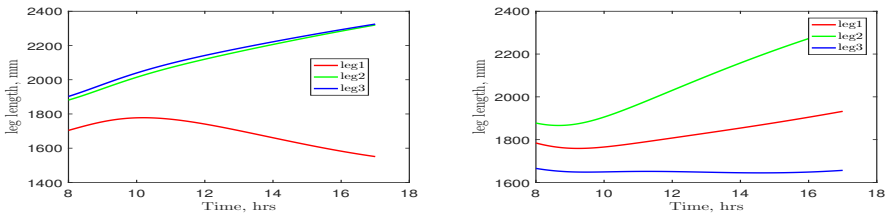

(a) Az-El (b) Az-El modified

Fig. 8: Actuations required for 3-UPU wrist in Az-El mode for summer solstice for Rajasthan

results obtained for modified Az-El method for summer solstice in Rajasthan. Here, the Az-El rotation matrix is multiplied with another rotation of 90° about the mirror normal to avoid intersection of the legs. Fig 8 gives the actuation

required for the 3-UPU heliostat in Az-El method in normal operation and when modified.

3.1. Spillage loss for 3-UPU wrist

From Fig 3, it can be seen that at some instants of time, the image goes out of the receiver aperture and this is often called as spillage loss. Fig 9 shows the spillage loss for various days for Bangalore. From these plots it is possible to find out at what time instant the switch from Az-El to T-A or vice-versa should be carried out from the point of view of reducing the spillage loss. As an example, for the March equinox (Fig 9a) and heliostat located as mentioned above the spillage loss in the T-A mode is less till 10:50 a.m. and for June solstice till 12.:40 p.m. Before these times the sun tracking can be done in the T-A mode and after these times the sun tracking should be switched to the Az-El mode. The analysis shown is for Bangalore, however similar simulations and analysis can be carried out for any other location on the Earth's surface and at any location in the heliostat field.

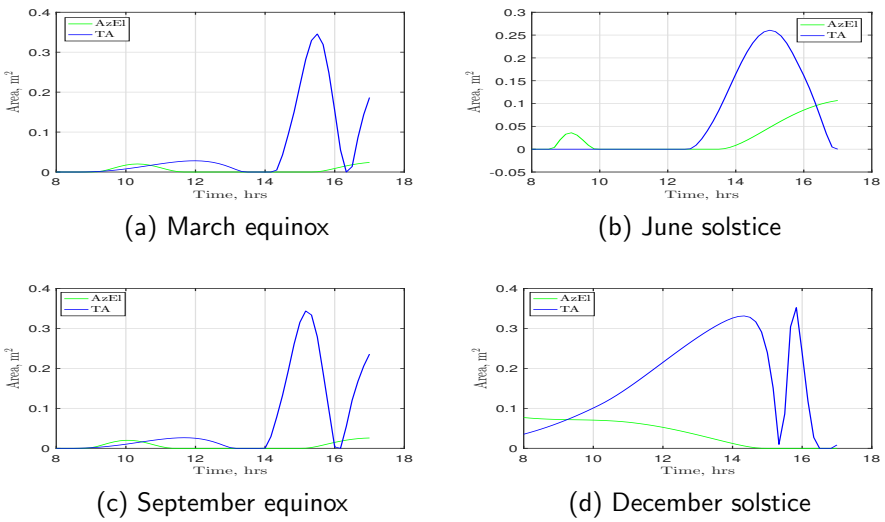

(a) March equinox (b) June solstice

(c) September equinox (d) December solstice

Fig. 9: Spillage loss for 3-UPU wrist for Bangalore

4. Experimental validation

4.1. Prototype design

With reference to Fig 10, the circum radii of the bottom and top platforms are chosen as 500 mm and 250 mm, respectively. The bottom platform which is equilateral, is attached with a 150° angle section at its corners. The U-joints are attached to this section thus giving the fixed point at a distance of 866 mm from

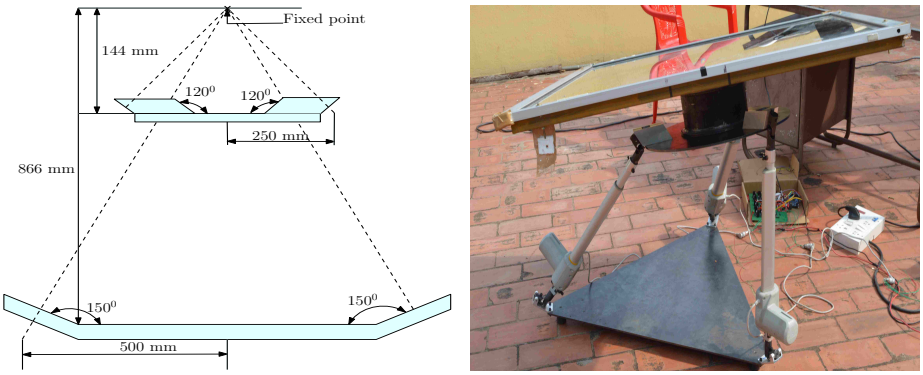

(a) Design parameters (b) Prototype

Fig. 10: The design parameters and the prototype of the 3-UPU wrist

the bottom. Similarly, the top platform has a 120° angle section attached to it. The mirror and the top platform are connected together using a cylindrical attachment (or a mirror rest as it is called in this work). The mirror rest has a diameter of 220 mm and a height of 138 mm. The mirror which has a dimension of 1 m × 1 m is supported at its back by a support structure to prevent it from excessive deflection due to wind loading or self-weight. The mirror rest along with the support structure is designed in such a way that the mirror centre coincides with the fixed point.

4.2. Control of 3-UPU manipulator

Closed loop [19, 20] as well as open loop control [24, 26] strategies are developed for the accurate tracking of Sun. Even though closed loop tracking algorithms are available, their rather tedious task of installing CCD cameras has forced the current industrial norm to be of open loop tracking. This is achieved by a periodic calibration using a target screen situated below the receiver aperture and image processing techniques. Here we employ open-loop control strategy relying on the predefined direction of Sun from algorithms already developed [25] and feedback from the actuator encoders. The actuators used to actuate the U-joints consist of a DC servo-motor connected to a lead screw. A full rotation of the motor shaft resulted in 1.5 mm translation, i.e., the pitch of the lead screw was 1.5 mm. The inertia of the motor, friction and other actuator parameters were not provided by the manufacturer. To obtain a transfer function of the linear actuator and find the actuator parameters, we performed experiments. For the actuator the input was a voltage and the output was the linear distance moved by the actuator. The rotation of the motor was measured from an inbuilt quadrature encoder. The input voltage was provided as a square wave of amplitude 20 V having a period of 10 s and 50 % duty cycle. An H-bridge was also used to reverse the motion of the actuator. We have

used MATLAB for system identification and estimating the transfer function. Typically the modeling of a DC motor is done using the equations 7 and 8

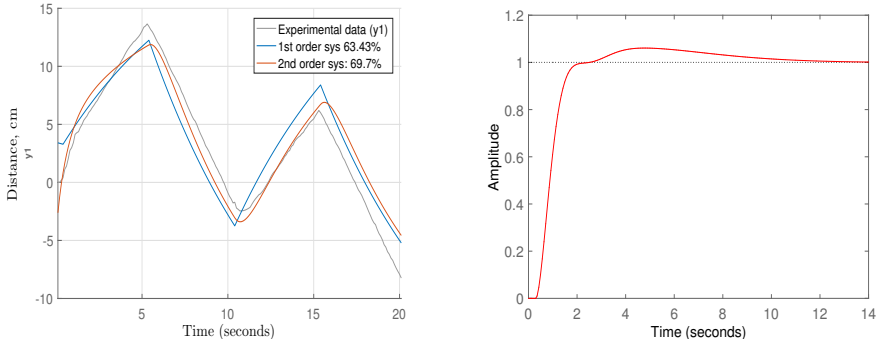

(a) System comparison (b) Step Response

Fig. 11: System identification using MATLAB-Simulink

$$L_a\dot{I}_a + R_aI_a = V - K\dot{\theta} \tag{7}$$

$$J\ddot{\theta} + b\dot{\theta} = Ki \tag{8}$$

The transfer function thus obtained by using the standard Laplace transform technique would be third order. If we assume that the value of inductance to be negligible, the system can be made simpler and also second order. Fig 11a gives the plot of experimental data (the encoder pulses converted to linear distance traversed which is obtained by multipying with a gain constant) versus the first order as well as second order system. It can be seen that the second-order system is more in accordance with the experimental data. The transfer function thus obtained using the system identification toolbox is given by Eqn. 9

$$H(s) = \exp^{-0.3s}\frac{0.2504}{s^2 + 1.759s + 0.2766} \tag{9}$$

It may be noted that the system identification results in an exponential term, $\exp^{-0.3s}$. This arises due to a delay between the given input and the output.

For this transfer function, a PID controller was developed in Simulink with a first-order filter on the derivative term given by Eqn. 10.

$$V(s) = K_p + \frac{K_i}{s} + K_d\frac{s}{1 + sT_f} \tag{10}$$

The value of the constants thus found out are $K_p = 6.43$, $K_i = 1.78$, $K_d = 4.34$, $T_f = 0.183$ and the step response plot for the estimated second order system is shown in Fig 11b. The tracking of Sun and reflecting the incident Sun rays to the receiver is carried out in discrete time intervals. The PID

controller with a settling time of 11 s would be suitable since the idle time between any two tracking instants would generally be in minutes. Once the system transfer function is obtained, we performed experiments on a roof top with the fabricated 3-UPU based heliostat. For the actual experiments, the co-ordinates of the centre of the receiver is at $[0\ 0\ 6.72]^T$ m with respect to the global co-ordinate system. The origin of the base co-ordinate system is at $[-10\ 3\ 0]^T$ m. For these chosen parameter values the translation at the P joints (also called leg lengths), to track the sun for May 24, 2017 and for Bangalore using the Az-El and the T-A methods discussed in section 2.3 is shown in Fig 12. The values of the leg lengths are the desired commands to an ATmega2560 micro-controller used to control the motion of the three actuators. Fig 13 shows the

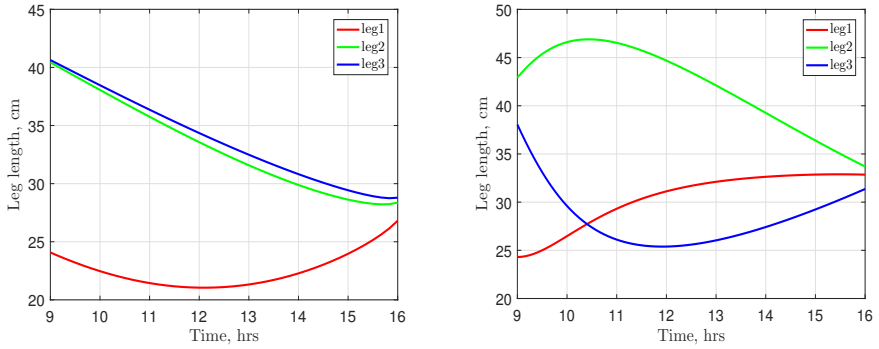

(a) Az-El mode (b) T-A mode

Fig. 12: Leg length required for the 3-UPU wrist to work in Az-El and T-A mode

image formed on the top of the tower for two time instants for both Az-El and T-A heliostats. As it can be seen from Fig 13, the 3-UPU based heliostat is able to track the sun in the Az-El and T-A mode. It can be seen that the two images on the receiver are separated and the difference in their location is somewhat large although the time interval between them is not very large. We discuss the possible sources of error in the next section.

4.3. Observations and discussions

One of the main problem with the sun tracking experiments carried out on the roof is that the fixed point on the heliostat is not exactly at 866 mm from the base. This is primarily the reason that the reflected image on the receiver is not at the aim point which is at the centre of the yellow rectangle (at 6.72 m from the global origin). A tighter manufacturing tolerance level has to be maintained for any future manufacturing.

As mentioned earlier, Sun tracking is done in discrete time intervals. This requires the heliostat to hold on to a particular orientation for a predefined period of time (or the actuators would be idle). During this time, if there are gusts

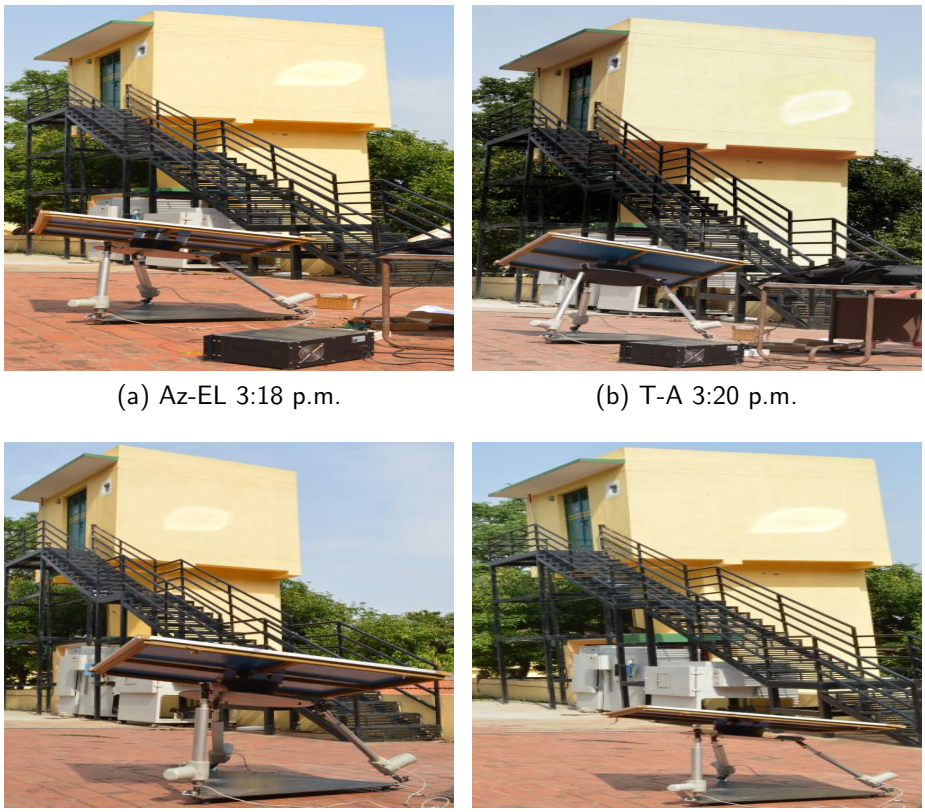

(a) Az-EL 3:18 p.m. (b) T-A 3:20 p.m.

(c) Az-EL 3:45 p.m. (d) T-A 3:48 p.m.

Fig. 13: The image on the receiver aperture at various time instants

strong enough to cause a change in the orientation of the mirror, the control system could not bring it back to its commanded location. This is referred to as instability in maintaining an orientation in the 3-UPU heliostat. An ideal 3-UPU-wrist should have only three degrees of freedom but the misalignment of the fixed point due to manufacturing inaccuracies makes it move in random manner in presence of gusts.

A second possible source of error is that fabricated prototype had some issues with stability in maintaining a particular orientation especially in presence of wind. A possible explanations could be that it deviates from the wrist conditions elaborated in [13] which is again due to manufacturing inaccuracies.

In spite of the errors, it can be concluded that the 3-UPU wrist heliostat is able to track the sun in both the Azimuth-Elevation and Target-Aligned mode. It may be mentioned that the switch between the two modes *does not* involve any hardware changes and can be simply done in software. In this sense, the 3-UPU based heliostat is reconfigurable and can be used in a mode where the

spillage losses and astigmatic aberrations can be minimized.

5. Conclusions and future work

This work presents the kinematic analysis, control and experimental validation of a novel 3-UPU wrist manipulator as a heliostat in CR systems. The existence of a fixed point for the 3-UPU wrist enables it to be used as an Az-El or a T-A heliostat by changing the control strategy alone and with absolutely no change in the hardware. The spillage losses can be minimized by switching from Az-EL to T-A or vice-versa. Extensive simulations have been carried out and this fact has been verified. The simulations have been verified using a prototype 3-UPU wrist manipulator based heliostat. The major advantage of using parallel manipulators as heliostats lie in its inherent ability to position the end-effector (mirror) more accurately thus improving the tracking accuracy when compared to serial mechanisms. Also, we can substitute rotary actuators and expensive gear reduction boxes with linear actuators with lead screw mechanism. Since there are three distributed supports, the deformation of the mirror under gravity and gusts would be minimum compared to serial mechanisms or in other words there is a possibility of using a bigger mirror.

The future work includes making a prototype with tighter manufacturing tolerances which will reduce the pointing errors as well as address the stability issues. Simulations for other potential locations on the surface of Earth and for various other days should be carried out. Finally, instead of the two configurations, rotations of the mirror about two arbitrary but independent axis can also be attempted to investigate if there are other better ways to use the available one degree of freedom redundancy.

References

[1] V. Gough, Contribution to discussion of papers on research in automobile stability, control and tyre performance, in: Proc. Auto Div. Inst. Mech. Eng, Vol. 171, 1956, pp. 392–394.

[2] D. Stewart, A platform with six degrees of freedom, Proceedings of the Institution of Mechanical Engineers **180** (1), 1965, pp. 371–386.

[3] J.-P. Merlet, Parallel robots, Vol. 74, Springer Science & Business Media, 2012.

[4] L. Vant-Hull, Concentrating solar power technology: Principles, developments and applications, Woodhead Publishing, Cambridge, UK, 2012, Ch. 8, pp. 240–283.

[5] A. Cammarata, Optimized design of a large-workspace 2-dof parallel robot for solar tracking systems, Mechanism and Machine Theory, **83**, 2015, pp. 175–186.

[6] O. Altuzarra, E. Macho, J. Aginaga, V. Petuya, Design of a solar tracking parallel mechanism with low energy consumption, Proceedings of the Institution of Mechanical Engineers, Part C: Journal of Mechanical Engineering Science, 2014, 0954406214537249.

[7] Google Inc., Heliostat cable actuation system design, Mountain View, California.

[8] W. Li, J. Sun, J. Zhang, K. He, R. Du, A novel parallel 2-dof spherical mechanism with one-to-one input-output mapping., WSEAS Transactions on Systems, **5** (6), 2006, pp. 1343–1348.

[9] C. M. Gosselin, F. Caron, Two degree-of-freedom spherical orienting device, US Patent 5,966,991, October 1999.

[10] M. Ruggiu, Kinematic and dynamic analysis of a two-degree-of-freedom spherical wrist, Journal of Mechanisms and Robotics, **2** (3), 2010, pp. 031006.

[11] M. Carricato, V. Parenti-Castelli, A novel fully decoupled two-degrees-of-freedom parallel wrist, The International Journal of Robotics Research, **23** (6), 2004, pp. 661–667.

[12] R. A. Shyam, A. Ghosal, Three-degree-of-freedom parallel manipulator to track the sun for concentrated solar power systems, Chinese Journal of Mechanical Engineering, **28** (4), 2015, pp. 793–800.

[13] M. Karouia, J. Hervé, A three-dof tripod for generating spherical rotation, in: Advances in Robot Kinematics, Springer, 2000, pp. 395–402.

[14] R. Di Gregorio, Kinematics of the 3-UPU wrist, Mechanism and Machine Theory, **38** (3), 2003, pp. 253–263.

[15] Y. Chen, K. Chong, T. Bligh, L. Chen, J. Yunus, K. Kannan, B. Lim, C. Lim, M. Alias, N. Bidin, et al., Non-imaging, focusing heliostat, Solar Energy, **71** (3), 2001, pp. 155–164.

[16] X. Wei, Z. Lu, W. Yu, H. Zhang, Z. Wang, Tracking and ray tracing equations for the target-aligned heliostat for solar tower power plants, Renewable Energy **36** (10), 2011, pp. 2687–2693.

[17] M. Guo, Z. Wang, W. Liang, X. Zhang, C. Zang, Z. Lu, X. Wei, Tracking formulas and strategies for a receiver oriented dual-axis tracking toroidal heliostat, Solar Energy, **84** (6), 2010, pp. 939–947.

[18] A. Ghosal, Robotics Fundamental Concepts and Analysis, Oxford University Press, New Delhi, India, 2006.

[19] Matteo Chiesi, Eleonora Franchi Scarselli and Roberto Guerrieri, Runtime detection and correction of heliostat tracking errors, Renewable Energy, **105**, 2017, pp. 702–711.

[20] F. J. Delgado, J. M. Quero, J. Garcia, C. L. Tarrida, P. R. Ortega, S. Bermejo, Accurate and wide-field-of-view mems-based sun sensor for industrial applications, IEEE Transactions on Industrial Electronics **59** (12), 2012, pp. 4871–4880.

[21] A. Pfahl, J. Coventry, M. Röger, F. Wolfertstetter, J. F. Vásquez-Arango, F. Gross, M. Arjomandi, P. Schwarzbözl, M. Geiger, P. Liedke, Progress in Heliostat Development, Solar Energy (In press, accepted manuscript), 2017.

[22] B.-H. Lim, K.-K. Chong, C.-S. Lim, A.-C. Lai, Latitude-orientated mode of non-imaging focusing heliostat using spinning-elevation tracking method, Solar Energy, 135, 2016, pp. 253–264.

[23] T. Ashley, E. Carrizosa, E. Fernández-Cara, Optimisation of aiming strategies in solar power tower plants, Energy (In press, accepted manuscript), 2017.

[24] R. Baheti, P. Scott, Design of self-calibrating controllers for heliostats in a solar power plant, IEEE Transactions on Automatic Control **25** (6), 1980, pp. 1091–1097.

[25] W. B. Stine, M. Geyer, Power from the Sun, Power from the sun. net, 2001.

[26] S. A. Jones, K. Stone, Analysis of solar two heliostat tracking error sources, Tech. rep., Sandia National Laboratories, Albuquerque, NM, and Livermore, CA, 1999.

[27] M. J. Lindberg V., Skf dual axis solar tracker-from concept to product, Chalmers University, Sweden.

[28] J. Freeman, B. Shankar, G. Sundaram, Inverse kinematics of a dual linear actuator pitch/roll heliostat, in: AIP Conference Proceedings, Vol. 1850, AIP Publishing, 2017, p. 030018.

[29] M. Balz, V. Göcke, T. Keck, F. von Reeken, G. Weinrebe, M. Wöhrbach, Stellio–development, construction and testing of a smart heliostat, in: AIP Conference Proceedings, Vol. 1734, AIP Publishing, 2016, p. 020002.

[30] F. Arbes, G. Weinrebe, M. Wöhrbach, Heliostat field cost reduction by slope driveoptimization, in: AIP Conference Proceedings, Vol. 1734, AIP Publishing, 2016, p. 160002.